Spatial resolution in rotating Spatial Encoding Magnetic field MRI (rSEM-MRI)

Clarissa Zimmerman Cooley[1,2], Jason P. Stockmann[1,3], Brandon D. Armstrong[1,3], Mathieu Sarracanie[1,3], Matthew S. Rosen[1,3], and Lawrence L. Wald[1,4]

[1]*A. A. Martinos Center for Biomedical Imaging, Dept. of Radiology, Massachusetts General Hospital, Charlestown, MA, United States,* [2]*Dept. of Electrical Engineering and Computer Science, Massachusetts Institute of Technology, Cambridge, MA, United States,* [3]*Dept. of Physics, Harvard University, Cambridge, MA, United States,* [4]*Harvard-MIT Division of Health Sciences and Technology, Cambridge, MA, United States*

TARGET AUDIENCE: MR system engineers and those requiring portable MRI systems.

PURPOSE: As the premiere modality for brain imaging, MRI could find wider applicability if lightweight, portable systems were available for siting in unconventional locations. However, realization of such lightweight, low power systems will require non-standard spatial encoding approaches such as rotating non-linear Spatial Encoding Magnetic fields (rSEMs). In this work we examine the spatial variations in image resolution of different SEMs for rotating scanners. We compare modeled spatial resolutions to acquired images encoded by a rotating SEM from a light-weight rotating Halbach magnet.

METHODS: A small rotating permanent magnet Halbach array with an inhomogeneous field has been used to create a portable 2D MRI scanner[1,2]. The field distribution, which is predominately quadrupolar (~320 Hz/cm^2), is used for image encoding instead of gradient coils. As the magnet is physically rotated around the object using a stepper motor, a RARE type spin echo sequence records the generalized projections onto the SEM. If sufficient multi-polar terms are present in the SEM, as is the case for the Halbach field, then parallel imaging is required to disambiguate the encoding[3]. We use a stationary 8 channel Rx array containing 8 cm overlapping loops whose sensitivity profiles vary with magnet rotation (as B_0 is rotated relative to the coils).

Data was acquired with the rotating Halbach scanner, and simulated for multiple rotating SEMs and simulation objects. These SEMs include the measured field of the Halbach magnet with and without an additional linear shim field (1.2mT/m), and a pure linear SEM with the same magnetic field range of the Halbach SEM (6 mT/m). In order to evaluate spatial resolution, a line of point sources spaced 5mm apart along the radius of the 16cm circular FOV were simulated. A 2D Gaussian low-pass filter was used to smooth the point sources to 0.5mm FWHM. In addition, images of single point sources were simulated to evaluate the varying FWHM of point spread functions (PSFs) along the radius.

Assuming a 20 KHz sampling BW, 256 point spin echoes were simulated for each coil and each magnet rotation (181 angles spaced 1^o apart). The phase accumulation with time in each voxel is calculated using the magnetic field map, then multiplied by the complex coil sensitivity map and the magnitude of the simulated object, and summed to form the net signal.

Data is reconstructed using the encoding matrix which contains the phase information estimated from the encoding field, as well as the effect of the coil sensitivities. This general encoding model is solved iteratively using the Algebraic Reconstruction Technique [2,4].

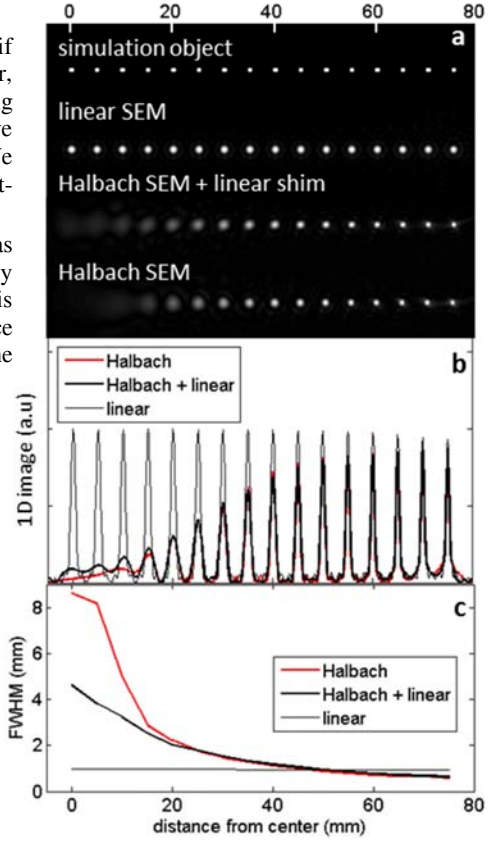

Figure 1: Simulated 2D (a) and 1D (b) images of a line of points starting at center of FOV using multiple rotating SEMs. (c) FWHM of the PSF along the radius. (x-axis common to fig. a,b, and c)

RESULTS: 2D and 1D images of a line of Gaussian points simulated from 3 rotating SEMs are shown in Figure 1a-b. Figure 1c shows variation in FWHM of simulated point spread functions along the radius. A uniform Rx coil was assumed for Fig. 1 simulations (the aliased portion is cropped). Simulated brain images using the 8 channel receive array, and the Halbach SEM or Halbach+linear SEM are shown in Figure 2 (noise levels matched to experimental data). Figure 3 shows experimental images using the Halbach SEM of a "MIT/MGH" phantom ($CuSO_4$-doped water, 1.7cm thick, 13cm dia.) acquired with 7 coils of the Rx array, 32 averages of a 6 spin echo train (TR = 550 ms, echo spacing = 8ms) and 91 2^o magnet rotations. Figure 4b shows a 1cm thick lemon slice imaged with 5 coils, a 128 echo train (TR = 4500ms, echo spacing = 8ms), and 181 1° magnet rotations.

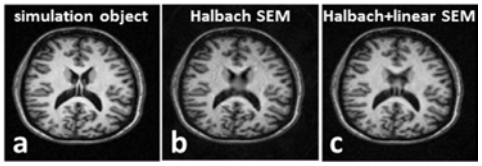

Figure 2: Simulations. (a) T1-weighted brain reference. (b) Simulated using Halbach SEM. (c) Simulated with Halbach SEM + linear field.

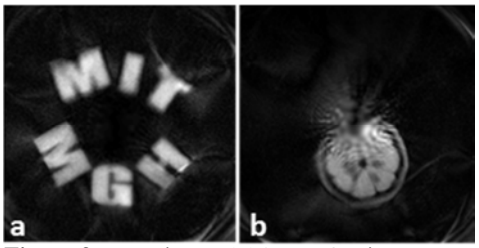

Figure 3: Experimental 16 cm FOV images. (a) 1.5cm thick phantom filled with CuSO4 doped water. (b) 1 cm thick lemon slice.

DISCUSSION & CONCLUSION: As expected, the resolution resulting from the rotating linear SEM is nearly uniform (Fig 1). Multi-polar SEMs have a steep gradient near the periphery and a shallow gradient near the center. This translates to the resulting resolution in images acquired with rSEMs with multi-polar components – higher resolution near the periphery and an "encoding hole" in the center (Fig 1, 2b, 3b). When a sufficient linear term is added to the SEM, the shallow encoding field region does not coincide with the axis of rotation. In this case, the "encoding hole" moves around the object resulting in less severe blurring (Fig 1, 2c). The simulations in Figure 2 show the theoretical resolution of the Halbach rSEM scanner when systematic errors are eliminated. These errors (effects seen in the experimental images, Fig. 3) likely result from field map or coil sensitivity profile inaccuracies propagating through the iterative reconstruction[6].

REFERENCES: (1) Zimmerman C, ISMRM 2012. (2) Cooley CZ, ISMRM 2013. (3) Schultz G, MRM 2010. (4) Gordon R, Journal of theoretical biology 1970. (6) Stockmann JP, MRM 2013.

ACKNOWLEDGMENTS: The authors thank C Lapierre, M Christensen, E Siskind, B Guerin, and S Cauley. Support by DoD/USAMRRA W81XWH-11-2-0076 (DM09094) and NIH P41EB015896.